



Fatal outcome after heart surgery in PMM2-CDG due to a rare homozygous gene variant with double effects

Marlen Görlacher^{a,1}, Eleftheria Panagiotou^{b,1}, Nastassja Himmelreich^a, Andreas Hüllen^a, Lars Beedgen^a, Bianca Dimitrov^a, Virginia Geiger^a, Matthias Zielonka^a, Verena Peters^a, Sabine Strahl^c, Jaime Vázquez-Jiménez^d, Gunter Kerst^b, Christian Thiel^{a,*}

^a Centre for Child and Adolescent Medicine, Department I, University Hospital Heidelberg, Heidelberg, Germany

^b Department of Pediatric Cardiology, University Hospital RWTH, Aachen, Germany

^c Centre for Organismal Studies (COS), Glycobiology, Heidelberg University, Heidelberg, Germany

^d Department of Pediatric Heart Surgery, University Hospital RWTH, Aachen, Germany

ARTICLE INFO

Keywords:

Congenital disorder(s) of glycosylation
PMM2
Phosphomannomutase 2
Splicing variant
Exon skipping
N-glycosylation

ABSTRACT

Variants in Phosphomannomutase 2 (PMM2) lead to PMM2-CDG, the most frequent congenital disorder of glycosylation (CDG). We here describe the disease course of a ten-month old patient who presented with the classical PMM2-CDG symptoms as cerebellar hypoplasia, retinitis pigmentosa, seizures, short stature, hepatomegaly, anaemia, recurrent vomiting and inverted mamillae. A severe form of tetralogy of Fallot was diagnosed and corrective surgery was performed at the age of 10 months. At the end of the cardiopulmonary bypass, a sudden oedematous reaction of the myocardium accompanied by biventricular pump failure was observed immediately after heparin antagonization with protamine sulfate. The patient died seven days after surgery, since myocardial function did not recover on ECMO support. We here describe the first patient carrying the homozygous variant g.18313A > T in the *PMM2* gene (NG_009209.1) that either can lead to c.394A > T (p. I132F) or even loss of 100 bp due to exon 5 skipping (c.348_447del; p.G117Rfs*4) which is comparable to a null allele. Proliferation and doubling time of the patient's fibroblasts were affected. In addition, we show that the induction of cellular stress by elevating the cell culture temperature to 40 °C led to a decrease of the patients' *PMM2* transcript as well as *PMM2* protein levels and subsequently to a significant loss of residual activity. We assume that metabolic stressful processes occurring after cardiac surgery led to the drop of the patient's *PMM* activity below a life-sustaining niveau which paved the way for the fatal outcome.

1. Introduction

Congenital disorders of glycosylation (CDG) are about 140 genetic defects in glycoprotein and glycolipid glycosylation as well as glycosaminoglycans and GPI-anchor synthesis ([19]; [8]). Within the protein *N*-glycosylation, PMM2-CDG (about 900 reported patients) is by far the most common CDG [22].

In PMM2-CDG (OMIM: 601785) the conversion of mannose-6-phosphate to mannose-1-phosphate by the cytosolic phosphomannomutase 2 (PMM2) is affected. This reduces GDP-mannose, an essential nucleotide-activated sugar substrate for the early steps in *N*-glycosylation [28]. This leads to the accumulation of shortened dolichol-linked oligosaccharides (Man₁₋₅GlcNAc₂-PP-Dol) and subsequently to reduced

provision of full-length dolichol-linked oligosaccharides (Glc₃Man₉GlcNAc₂-PP-Dol) needed for the transfer onto the nascent glycoprotein by the oligosaccharyl transferase complex. As a consequence, glycosylation sites on glycoproteins are partially non-occupied by *N*-glycans leading to protein *N*-hypoglycosylation, indicated by a CDG type 1 pattern of serum transferrin after isoelectric focusing or HPLC separation.

PMM2-CDG is a multisystem disease including neurological involvement and variable dysmorphism such as prominent forehead, long face, epicanthal folds, almond-shaped eyes, short nose, anteverted nares, long philtrum, thin upper lip, high-arched palate, large and protruding ears, microcephaly or macrocephaly, abnormal fat pads, inverted mamillae and cryptorchidism in boys [1]. The severity of the clinical presentation is mainly attributed to the patient's biallelic variant status

* Corresponding author at: Centre for Child and Adolescent Medicine, Pediatrics I, University of Heidelberg, Heidelberg, Germany.

E-mail address: Christian.thiel@med.uni-heidelberg.de (C. Thiel).

¹ Görlacher & Panagiotou contributed equally.

and thus the residual activity of PMM2.

PMM2 is a 28 kDa protein (NP_000294.1) encoded by 741 bp (NM_000303.3). The *PMM2* gene (NG_009209.1) comprises eight exons and spans about 20 kbp on chromosome 16p13.2. Nearly 200 intronic and exonic variants are already associated with PMM2-CDG (see NCBI, ClinVar: <https://www.ncbi.nlm.nih.gov/clinvar>), most of them result in amino acid substitutions affecting the enzymatic conversion of mannose-6-phosphate or the stability of the protein.

Here we describe the first PMM2-CDG patient with homozygosity for variant NG_009209.1:g.18313A > T which provokes two effects: shortening of the protein length by exon splicing and an amino acid alteration of the PMM2 protein composition due to a nucleotide substitution.

2. Materials and methods

2.1. Patient material

The study was performed in accordance with the Declaration of Helsinki and approved by the Ethics Committees of the Medical Faculty Aachen. Written informed consent was obtained from the parents for biochemical and sequencing analysis. The parents also consented to molecular testing (Sanger sequencing) of their own PMM2 status. Written informed consent was also obtained for the use of clinical information.

2.2. Isoelectric focusing and SDS-PAGE of serum transferrin

Isoelectric focusing of serum transferrin was carried out as described by Niehues and co-workers [20].

2.3. Cell culture and cell collecting

Patient and control fibroblasts were cultured in Dulbecco's modified Eagle's medium (high glucose, Life Technologies) supplemented with 10% fetal calf serum (PAN Biotech) and 1% Pen/Strep at 5% CO₂ at 37 °C. Growth medium was changed every 72 h. Two days before running the assays, 2 × 10⁶ fibroblasts were seeded and cultivated under the above-mentioned conditions at 37 °C and 40 °C, respectively. After 48 h cells were collected by scraping and used for the isolation of proteins and total RNA.

2.4. PMM and MPI activity assay

PMM activity was determined in control and patient fibroblasts. To isolate proteins, the scraped cells were solubilized (50 mM Hepes, pH 7.1) and centrifuged (45 min at 45,000 rpm and 4 °C). 30 µg of protein from the supernatant was used for the assay. PMM activity was determined via a coupled photometric assay at 340 nm for 120 min as described [14]. The photometric assay was performed at 37 °C and 40 °C, respectively. The MPI activity was also performed in a photometric assay with 30 µg protein as described [20].

2.5. Analysis of dolichol-linked oligosaccharides

1 × 10⁶ fibroblasts derived from a control and the patient were cultured, and labelled with [2-³H]mannose for 30 min. Dolichol-linked oligosaccharides (LLO) were extracted and analysed by HPLC [27].

2.6. SDS-PAGE and Western blot

SDS-PAGE (10%) and Western blot were performed with the same protein material isolated for the PMM activity assay (see above). 10 µg of protein of the patient and controls were used per lane. Further procedure was as described previously [11]. All antibodies were diluted in PBS-T (0.1% Tween in PBS). Primary antibodies used were anti-PMM2 (rabbit anti human, polyclonal; Proteintech) in a 1:1000 dilution and anti-

β-actin (mouse anti human; polyclonal, Sigma-Aldrich) in a 1:10,000 dilution. As secondary antibodies we used anti-rabbit IgG conjugated with horseradish peroxidase (HRP) for PMM2 detection (Santa Cruz) and anti-mouse IgG-HRP for β-actin (Santa Cruz). Both secondary antibodies were diluted 1:10,000 in PBS-T. Protein signals were detected by light emission with Pierce™ ECL Western blotting substrate. Quantification of signal strength was performed by using ImageJ (www.imagej.nih.gov).

2.7. Variant analysis in PMM2

Total RNA was extracted from control and patient fibroblasts (incubated at 37 °C) using the RNeasy kit (Qiagen). First strand cDNA of *PMM2* (NM_000303.3) was synthesized from 0.5 µg of total RNA with Omniscript reverse transcriptase (Qiagen) and the primer hPMM2_R1 (5'-GACTGCACATGCCTGGCATAG-3'). In a first round of PCR the cDNA was amplified with primers PMM2_F1 (5'-CGGAAGTCCGGGCCGAGT-3') and PMM2_R1 by using the HotStar-Taq-Polymerase kit (Qiagen). In a nested PCR, primers were PMM2_F2 (5'-CTCGTGCCAAACGTGTCTTGTGTA-3') and PMM2_R2 (5'-GCAGAGCTGCCTAGGCTG-3'). Thermo Cycler conditions were: 94 °C for 1 min, followed by 35 cycles with 94 °C for 30 s, 55 °C for 30 s and 72 °C for 1.5 min.

Genomic DNA from control and patient fibroblasts was isolated with the Genomic DNA Isolation Kit (Sigma-Aldrich). 100 ng of genomic DNA was used for amplification of *PMM2* exon 5 (NG_009209.1) in two rounds of PCR with primers PMM2_Ex5-6_F1 (5'-GCTGAGAAA-CATTGACCACACT-3') together with PMM2_Ex5-6_R1 (5'-CATA-C TTCATTATCAATAGCTCAC-3') and PMM2_Ex5-6_F2 (5'-GCTGTT TATCTATGATGTTGCCAA-3') paired with PMM2_Ex5-6_R2 (5'-TGGGTATCCAAGTTTGGAAACAC-3') under the above-mentioned conditions. cDNA and exon PCR products were separated on 1% agarose gels and fragments were isolated with the peqGOLD (PeqLab) gel extraction kit. Variant analysis was performed by Sanger sequencing. The variant was uploaded to ClinVar Submission Wizard (SUB6890963; www.ncbi.nlm.nih.gov/clinvar/).

2.8. Quantitative real-time PCR (qRT-PCR)

Total RNA was extracted from patient and control fibroblasts incubated at 37 °C and 40 °C using the MasterPure RNA purification kit (Epicentre Biotechnologies). One µg of RNA was reverse transcribed using random hexamer primers (Invitrogen) and the RevertAid Reverse Transcriptase (Thermo Scientific). Quantitative real-time PCR was performed with SensiFAST SYBR No-ROX-Mix (Bioline) with 50 ng cDNA in a CFX Connect Real-Time System (Bio Rad) with the following parameters: step 1: 95 °C, 15 s; step 2: 95 °C, 15 s; step 3: 60 °C, 1 min; step 4: 72 °C 10 s; step 5: 65 °C to 100 °C, 5 min; step 6: hold on 4 °C. Steps 2–4 were repeated 35 times. Primers were qPCR_PMM2_Ex5-8_F (5'-TGTCCTTATTGGAAGAAGC-3'), qPCR_PMM2_Ex5-8_R (5'-GATCTCATGGTCATTGCC-3') and qPCR_PMM2_Ex6-8_F (5'-CAGATCTACGAAAGAGT3') together with qPCR_PMM2_Ex6-8_R (5'-GATCTCATGGTCATTGCC3'). *PMM2* expression was normalized against the gene expression of *Ras-related protein (RAB7A)* by using primers RAB7A_qPCR_F (5'-TGGGAGATTCTGGAGTCGGG-3') combined with RAB7A_qPCR_R (5'-CACACCGAGAGACTGGAACC-3').

2.9. Immunofluorescence studies

One day before preparation, 6 × 10⁴ fibroblasts were seeded on glass cover slips. Immunofluorescence was carried out as described (Hansske et al., 2001). Cells were stained with antibodies against PMM2 (Proteintech, rabbit anti-human, 1:400 in PBS-T) and MPI (Sigma Aldrich, mouse anti-human, 1:500). After incubation with fluorochrome-conjugated secondary antibodies (Alexa Fluor 488, ThermoFisher, goat anti-rabbit, 1:500; Alexa Fluor 568, ThermoFisher, goat anti-mouse, 1:500), respectively, cells were mounted with Mowiol and analysed by confocal fluorescence microscopy.

2.10. Cell proliferation studies by live cell monitoring

Cell proliferation was assessed by following the manufacturer's guidelines using the XCelligence device (ACEA Biosciences). We seeded 1000 cells to the measuring cavities and cultured them under standard conditions for 120 h. Cell density was computer-based recorded every 30 min. Quantification was carried out with slope values (1/h) measured during the logarithmic growth phase according to the manufacturer's guidelines.

2.11. Statistics

With exception of the LLO analysis, all experiments have been repeated at least three times. Data were analysed using Student's *t*-test for single comparisons or one-way ANOVA followed by Bonferroni's test for multiple comparisons. Significances of *p* values: **p* ≤ 0.05; ***p* ≤ 0.005; ****p* ≤ 0.001. Data are displayed as means ± standard deviation (SD).

3. Results

3.1. Patient report

This 10 month-old boy from related Turkish parents was referred for treatment of tetralogy of Fallot with severely hypoplastic infundibulum, pulmonary valve and pulmonary artery branches (Fig. 1). The patient showed also a small stature, inverted mamillae, bilateral radial aplasia, right-sided clubfoot, left-sided drop foot, retinitis pigmentosa, hepatosplenomegaly, cerebellar hypoplasia, reduced signals in the T2 sequence in consensus with white matter abnormality and generalized muscular hypotonia. Laboratory findings showed thrombocytopenia and increased serum transaminases. Because of recurrent hypoxemic spells, a modified Blalock-Taussig-shunt was placed at the age of six weeks. The postoperative course was uneventful. The boy showed neither thrombotic nor bleeding complications on standard antiplatelet therapy. At six months of age, a balloon angioplasty of the shunt and the hypoplastic pulmonary valve was performed. Corrective surgery at this time was not performed because the boy showed significant comorbidities: recurrent vomiting, leading to a failure to thrive, seizures necessitating anticonvulsive therapy and a presumably viral encephalitis. Corrective surgery was postponed until ten months of age and after this surgery and during weaning from cardiopulmonary bypass, transesophageal echocardiography (TOE) showed no residual defects and a good biventricular function. In order to reverse the anticoagulant effects of heparin at the end of the surgery, protamine sulphate was administered. Shortly after,



Fig. 1. Intra-operative transesophageal echocardiography showed significant hypertrophy with increased septum thickness. Numbers indicate the penetration depth of echo in cm.

intensified catecholamine support was needed to stabilize the patient. TOE revealed increasing thickening of the myocardium of both ventricles compatible with biventricular edema and a severely reduced biventricular function, possibly due to microthrombotic cardiac ischemia. The patient was put on cardiopulmonary support by extracorporeal membrane oxygenation (ECMO). However, due to persistent non-recovery of biventricular function followed by multiorgan failure the boy died seven days after surgery. In respect to the multiple morphological stigmata and the unusual clinical course after cardiac surgery, diagnostic laboratory tests were initiated.

3.2. Isoelectric focusing of serum transferrin revealed a CDG-I pattern

Initial CDG diagnostics was conducted by isoelectric focusing of serum transferrin which revealed a CDG type 1 pattern (Fig. 2A: elevated asialotransferrin (8%, ref. val. 0% - 2%) and disialotransferrin (16%, ref. val. 5% - 13%), and decreased tetrasialotransferrin (21%, ref. val. 30% - 55%; see [7] for ref. values)).

3.3. Sanger sequencing of the PMM2 gene identified a rare homozygous variant

Analysis of the patient's *PMM2* gene by Sanger sequencing showed the homozygous variant NG_009209.1:g.18313A > T in exon 5. Both parents are carriers for the mutation. Interestingly, on cDNA level two different effects were provoked. First, base exchange c.394A > T leads to amino acid substitution p.I132F (Fig. 2B). Second, exon 5 was spliced out, whereby 100 bp (c.348-447 bp) were skipped and the *PMM2* open reading frame was significantly altered (Fig. 2C and D). Concerning the amino acid substitution, isoleucine 132 is a highly conserved amino acid from *Homo sapiens* to *Xenopus tropicalis* (Fig. 2D), indicating its important role for function. Regarding the loss of 100 bp by deletion of exon 5, three alternative amino acids would be introduced after arginine 116. The patient's *PMM2* would then be terminated due to a premature stop codon (Fig. 2E), leading to a protein with a theoretical molecular weight of 13.5 kDa (correlating with a loss of 51% of the wildtype protein size).

3.4. Reduced PMM activity due to diminished PMM2 protein and reduced PMM2 transcript levels

The PMM activity in fibroblasts at the physiological relevant 37 °C was significantly reduced to 7.4% (± 1.3%; *n* = 6; ****p* < 0.001; controls (100.0% ± 22.6%)) (Fig. 2F). MPI activity was normal (data not shown).

In Western blot analysis of fibroblasts, the patient's *PMM2* expression was significantly reduced to 19.4% (± 11.8%; *n* = 6; ****p* < 0.001; controls (100.0% ± 23.8%)) (Fig. 2G). Notably, no additional protein band was observed at 13.5 kDa in the patient. We also like to mention that the localization of the patient's *PMM2* was not affected since it colocalizes with the cytosolic MPI in immunofluorescence analysis. Also, it was not mislocalized into the nucleus (data not shown). To further elucidate whether the PMM activity reduction was due to an impact on the patient's *PMM2* mRNA level, qRT-PCR studies were performed. Normalized to *RAB7* of the control (103.0% ± 27.0%), the quantity of the patient's *PMM2* mRNA of the missense variant carrying transcript was significantly diminished (47.0% ± 8.5%; *n* = 9; ****p* ≤ 0.001) (Fig. 2H). Additional qPCR analyses of the transcript with loss of exon 5 revealed almost the same significant reduction of mRNA expression level (42.0% ± 7.0%; *n* = 9; ****p* ≤ 0.001) (data not shown). Next, we analysed the cells' doubling time and proliferation. Comparison of the slope values measured during the logarithmic growth phase (between 55 h to 110 h) showed that the patient's fibroblasts needed 1.25 times longer doubling time (29.9 h ± 1.8 h) than the control (23.9 h ± 0.3 h; *n* = 3; ****p* ≤ 0.002; Fig. 2J). Besides, the proliferation of the patient's fibroblasts (0,017 ± 0,004) was significantly reduced to 44.7% ± 10.5% (controls 0,038 ± 0,004; *n* = 3; ****p* ≤ 0,002) (Fig. 2K).

Putting stress on the cells by incubating them at 40 °C and repeating

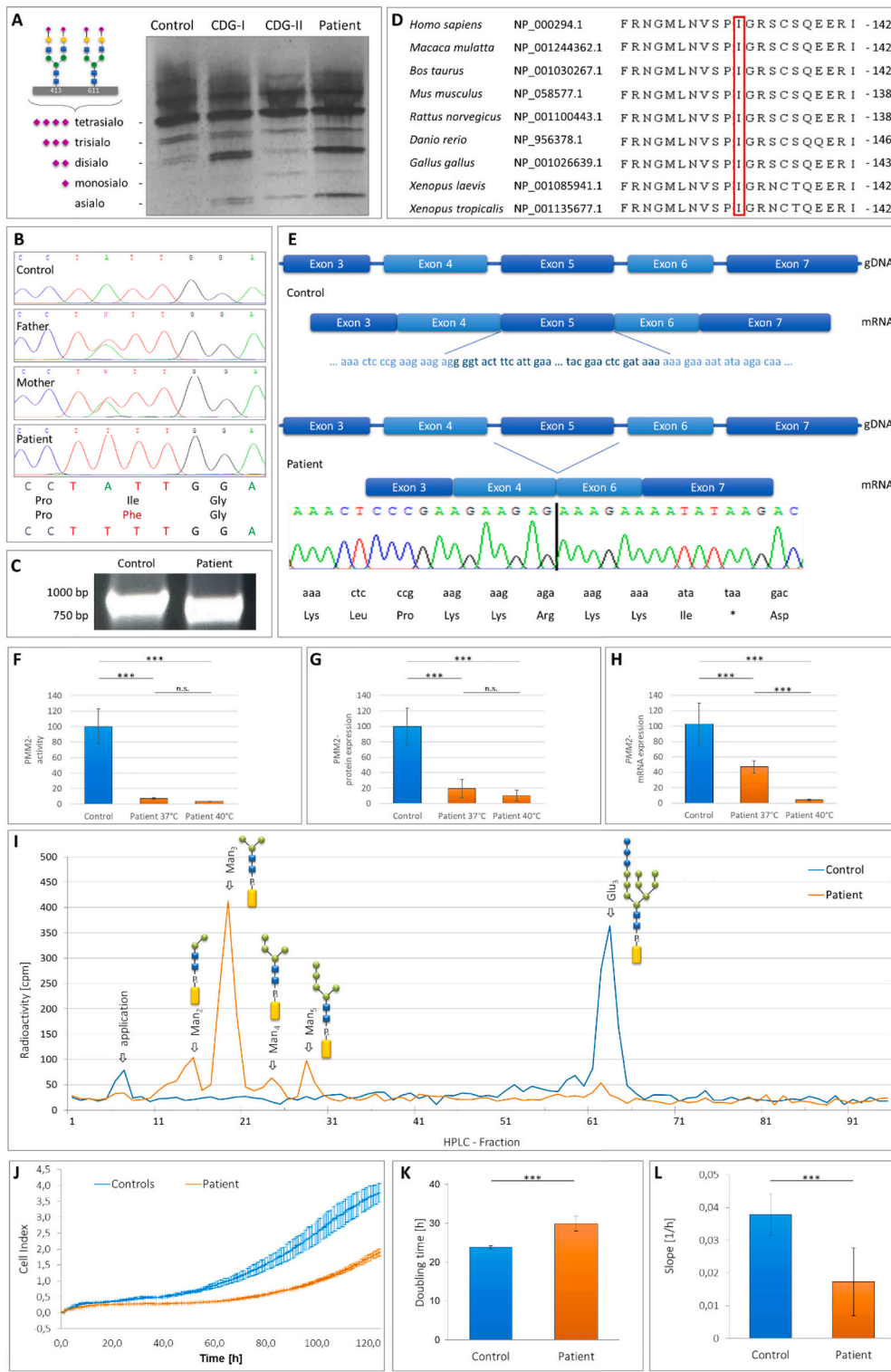


Fig. 2. A Isoelectric focussing of serum transferrin revealed elevated amounts of disialo- and asialotransferrin in case of the patient (lane 4), indicating a CDG-I disease. As internal standards also a healthy control (lane 1) and CDG-I (lane 2) as well as CDG-II patients' samples (lane 3) are included. B Sanger Sequencing of *PMM2* exon 5 showed homozygosity for variant c.394A > T (p. I132F) in the patient. The parents are heterozygous carriers. C Due to the loss of exon 5, amplification of the *PMM2* cDNA by RT-PCR revealed a 100 bp shorter PCR product in case of the patient than in the control. D *PMM2* protein alignment demonstrated Ile¹³² as a highly conserved amino acid in a highly conserved stretch through different species. E Schematic intron-exon structure of *PMM2* from exon 3 to exon 7 (gDNA) and the spliced mRNA fragment (mRNA) of a healthy control and the patient with deletion of exon 5 leading to a shift in the open reading frame and a mutated C-terminus ending in Lys-Lys-Arg-Lys-Lys-Ile-* (short: KKRKKI*). F *PMM2* activity analysis of a control and the patient. At 37 °C the patient's activity was reduced to 7%, whereas at 40 °C, the activity was only 3% as compared to the value measured at 37 °C. G Western blot analysis for *PMM2* of control and patient fibroblasts. In comparison to the control, the patient's *PMM2* expression was clearly reduced to 19% at 37 °C and further declined to 10% at 40 °C. H *PMM2* qRT-PCR studies of control and patient fibroblasts. At 37 °C the *PMM2* expression in the patient cells was diminished to 47% compared to the control, whereas only 4% residual *PMM2* transcript level could be detected at 40 °C in case of the patient. I HPLC analysis of LLOs derived from control (in blue) and patient's fibroblasts (in orange) after metabolic labelling with [2-³H]mannose displayed accumulations of shortened oligosaccharide structures Man₂₋₅ (Man₂₋₅GlcNAc₂-PP-Dol) accompanied by depletion of the full-length oligosaccharide Glc₃. (Glc₃Man₉GlcNAc₂-PP-Dol). J – L Analysis of cell growth. (J) XCelligence device analysis of cell proliferation of a control (blue) and the patient (orange) measured over 5 days. (K) *PMM2*-deficient cells needed about 1,25 times longer for doubling compared to control fibroblasts and showed a significantly reduced cell proliferation (L). Used symbols: ■ = dolichol, ● = galactose, ■ = N-Acetylglucosamine, ● = mannose, ● = glucose, ◆ = sialic acid

the analyses on the transcript and protein level, we found that the patient's PMM2 protein expression dropped by 53.1% to 10.3% ($\pm 6.9\%$; n.s.) in comparison to the data measured at 37 °C (Fig. 2G). This phenomenon was accompanied by an almost equivalent loss (minus of 54.1%) of PMM activity to 3.4% ($\pm 0.3\%$; $n = 6$; $***p < 0.001$) (Fig. 2F). Additionally, our qRT-PCR analysis revealed that due to the temperature increase in cell culture, the patient's PMM2 missense variant carrying transcript declined to 4.0% ($\pm 0.3\%$; $n = 9$; $***p < 0.001$) which is equal to a minus of 91.5% in comparison to the amount measured at 37 °C (Fig. 2H). Concerning the patient's PMM2 transcript level without exon 5, we detected 7.0% ($\pm 2.7\%$; $n = 9$; $***p < 0.001$; data not shown). In addition, LLO analysis revealed significant accumulations of shortened dolichol-linked oligosaccharides (esp. Man₃₋₅GlcNAc₂-PP-Dol; Fig. 2I), pointing to a severe impact of the patient's PMM2 deficiency on the early steps of glycoprotein biosynthesis.

4. Discussion

The present patient was homozygous for the variant NG_009209.1:g.18313A > T in exon 5 of the PMM2 gene. To our knowledge this is the first time that homozygosity for this variant was found. Accordingly, database search revealed no entry in e.g. ClinVar or Ensemble. We found only one patient in the literature who was compound-heterozygous for c.394A > T (p.I132F) and c.338C > T (p.P113L) [17]. The closely related variant c.395 T > C (p.I132T) was found in 12 patients and was then associated with c.422G > A (p.R141H; 7 cases; Matthijs et al., 1998; [6,17,29]), c.368G > A (p.R123Q; 3 cases; [4,6,17,29]), c.620 T > C (p.F207S; 1 case, [24]) and c.58C > T (p.P20S; [17]). These patients consistently showed a severe phenotype. There is no information available about premature deaths.

On the cDNA level, we found that variant NG_009209.1:g.18313A > T leads to c.394A > T and subsequently to amino acid exchange p.I132F but as well to pseudosplicing of 100 bp (c.348_447del; p.G117Rfs*4) which comprised the complete exon 5 of the PMM2 gene. This is in accordance with a former study on a compound-heterozygous patient (c.394A > T and c.338C > T) showing that NG_009209.1:g.18313A > T was a splicing enhancer sequence [17]. Due to the exon loss and the subsequent shift in the open reading frame, a significantly shortened PMM2 protein of 13.5 kDa would be generated in which amino acids glycine 117, threonine 118 and phenylalanine 119 are changed into lysine 117, lysine 118 and isoleucine 119 before a premature termination occurred. Thereby this mutated protein would end in a KKRKK(I*) sequence, a single (monopartite) stretch of basic amino acids which displays a consensus motif for a nuclear localization signal in heat shock events [16]. However, we neither detected the shortened 13.5 kDa PMM2 by Western blot nor in the nucleus by immunofluorescence studies which indicates that it was not present. Whether already the shortened mRNA was degraded by nonsense mediated mRNA decay or the truncated protein by the unfolded protein response as quality control system of the cell, remains outside the scope of this manuscript. In addition, due to the fact that amino acids arginine123, arginine134 and arginine141 which are needed for substrate binding of GDP-mannose at the active side of the enzyme would be affected [2], we estimate that this protein would have had no activity. This is in line with experimental data for the most common amino acid substitution (p.R141H) in PMM2-CDG, originating from another base pair variant in exon 5, which leads to a protein with no enzymatic activity [13]. According to Andreotti and coworkers [2], p.I132F does not affect the active site of PMM2. Besides, the structural prediction of the PMM2 dimer by PDBePISA [15] indicates that variant p.I132F is buried in the structure and is not found at the protein interface (supplementary figure). However, computational simulation with DynaMut [23] predicts a destabilization of the protein ($\Delta\Delta G$: -0.492 kcal/mol) and hence supports the assumption that the homozygous mutation p.I132F reduces both, the protein dynamics and the stability resulting from vibrational entropy changes (supplementary figure). Although two differently

mutated PMM2 proteins can form heterodimers where one subunit stabilizes the other in a complementary fashion [3], we assume that this kind of dimerization is prevented in the presented patient due to homozygosity of variant p.I132F, which might be an additional explanation for the severity of this case. As the low residual PMM activity (7%) in the patient's fibroblasts arose from the full-length PMM2 protein carrying the p.I132F substitution only, we rate it as one of the severe PMM2 mutations [18,30].

Inflammation, remodelling and proliferation are important process in wound healing. This begins between day 4 and 5 after injury or surgery with the migration of fibroblasts into the wound matrix [26]. Since we found that the cell doubling time was significantly enhanced which was accompanied by a significantly reduced proliferation rate, we expect a general impact on the course of the healing.

It is well known that surgery can lead to wide and severe metabolic disarrangements as increased oxygen and energy consumption, hormonal imbalance, hyperglycaemia, hyperlactatemia, increased glutamate, aspartate and free fatty acid concentrations as well as increased systemic inflammation [9,12]. More recent studies even showed that after cardiac surgery extensive changes in the N-glycosylation of total plasma proteins are initiated within the first three days after the onset of the normal systemic inflammation [21]. Although this glycan-dependent mechanism is not completely understood, it nonetheless emphasises the importance of a functional glycosylation machinery during the stressful period of healing.

No plasma or serum sample was taken during surgery to test for respective N-glycan changes. But when we put stress on the patient's fibroblasts by elevating the incubation temperature to 40 °C, we significantly reduced the PMM2 transcript and protein level. Strikingly, the residual PMM2 activity hereby fell to 3.4%. Since fibroblasts generally show higher activities then, for example, leukocytes [10], one cannot rule out an even more severe effect of hyperthermia on the activity in other organs. However, a surgical wound and its surrounding exhibit a significant increase in wound temperature [25]. So, we suppose that at least the heart region around the surgery scar was impacted by an extremely low PMM2 activity, being insufficient for the glycosylation-dependent curing and proliferation processes which in combination could have led to the patient's bad outcome at day 7 after surgery.

Protamine is an antidote routinely used to antagonize the heparin effect after surgery. Whether the patient's strong response to protamine administration during weaning from the cardiopulmonary bypass was directly related to the PMM2 glycosylation defect, is unclear. Reports with experiences from surgeries of other CDG patients are rare. However, protamine administration itself is associated with immunological and inflammatory alterations, and may induce an anaphylactic response with hypotension, bradycardia, pulmonary vasoconstriction, and allergy [5].

In conclusion, we consider homozygosity for the variant NG_009209.1:g.18313A > T to be life threatening, not only during surgery but also during a normal infection with fever, due to the temperature sensitivity of PMM2 transcripts. Since the majority of PMM2-CDG variants are not completely biochemically studied, more studies esp. under hyperthermia conditions are needed. Besides, a moderate cooling of the surgery area should be considered as potential benefit for (CDG) patients carrying thermolabile variants. Moreover, due to potential side-effects during surgeries, replacement of heparin and protamine application by e.g. bivalirudin, a direct thrombin inhibitor, should be considered for patients suffering from CDG or other severe metabolic defects.

Supplementary data to this article can be found online at <https://doi.org/10.1016/j.ymgmr.2020.100673>.

Funding

This study was supported by the Deutsche Forschungsgemeinschaft

(DFG, German Research Foundation; Forschungsgruppe FOR 2509, Project-ID TH1461/7–1 to CT and STR 443/6–1 to SS) and the European Commission (E-Rare-3 Joint Transnational Call 2018/ EUROGLYCAN-OMICS in association with the Deutsche Forschungsgemeinschaft, Project-ID TH1461/9–1).

Contributions

MG: Planned and conducted experiments, contributed to the writing of the manuscript. NH, AH, LB, BD, VG: Conducted experiments. EP, GK, MZ, VP, SS, JVJ: Collected data and contributed to the interpretation of the results. CT: Planning of experiments, interpretation of data and writing of the manuscript.

Declaration of Competing Interest

The authors declare that there is no conflict of interests.

References

- [1] R. Altassan, R. Péanne, J. Jaeken, et al., International clinical guidelines for the management of phosphomannomutase 2-congenital disorders of glycosylation: diagnosis, treatment and follow up, *J. Inherit. Metab. Dis.* 42 (2019) 5–28.
- [2] G. Andreotti, I. Cabeza de Vaca, A. Poziello, M.C. Monti, V. Guallar, M.V. Cubellis, Conformational response to ligand binding in phosphomannomutase2: insights into inborn glycosylation disorder, *J. Biol. Chem.* 289 (2014) 34900–34910.
- [3] G. Andreotti, M.C. Monti, V. Citro, M.V. Cubellis, Heterodimerization of two pathological mutants enhances the activity of human phosphomannomutase2, *PLoS One* 10 (2015), e0139882.
- [4] J.B. Arnoux, N. Boddaert, V. Valayannopoulos, et al., Risk assessment of acute vascular events in congenital disorder of glycosylation type Ia *Mol. Genet. Metab.* 93 (2008) 444–449.
- [5] C. Boer, M.I. Meesters, D. Veerhoek, A.B.A. Vonk, Anticoagulant and side-effects of protamine in cardiac surgery: a narrative review, *Br. J. Anaesth.* 120 (2018) 914–927.
- [6] P. De Lonlay, N. Seta, S. Barrot, et al., A broad spectrum of clinical presentations in congenital disorders of glycosylation I: a series of 26 cases, *J. Med. Genet.* 38 (1) (2001) 14–19, <https://doi.org/10.1136/jmg.38.1.14>.
- [7] B. Dimitrov, N. Himmelreich, A.L. Hipgrave Ederveen, et al., Cutis laxa, exocrine pancreatic insufficiency and altered cellular metabolomics as additional symptoms in a new patient with ATP6AP1-CDG, *Mol. Genet. Metab.* 123 (2018) 364–374.
- [8] C.R. Ferreira, C.D.M. Van Karnebeek, J. Vockley, N. Blau, A proposed nosology of inborn errors of metabolism, *Genet Med.* 21 (2019) 102–106.
- [9] C.C. Finnerty, N.T. Mabvuure, A. Ali, R.A. Kozar, D.N. Herndon, The surgically induced stress response, *JPEN J. Parenter. Enteral Nutr.* 37 (2013), 21S-9S.
- [10] S. Grünwald, E. Schollen, E. Van Schaftingen, J. Jaeken, G. Matthijs, High residual activity of PMM2 in patients' fibroblasts: possible pitfall in the diagnosis of CDG-Ia (phosphomannomutase deficiency), *Am. J. Hum. Genet.* 68 (2001) 347–354.
- [11] N. Himmelreich, B. Dimitrov, V. Geiger, et al., Novel variants and clinical symptoms in four new ALG3-CDG patients, review of the literature, and identification of AAGRP-ALG3 as a novel ALG3 variant with alanine and glycine-rich N-terminus, *Hum. Mutat.* 40 (2019) 938–951.
- [12] S.M. Jakob, H. Ensinger, J. Takala, Metabolic changes after cardiac surgery, *Curr Opin Clin Nutr Metab Care.* 4 (2) (2001 Mar) 149–155.
- [13] S. Kjaergaard, F. Skovby, M. Schwartz, Carbohydrate-deficient glycoprotein syndrome type 1A: expression and characterisation of wild type and mutant PMM2 in *E. coli*, *Eur. J. Hum. Genet.* 7 (1999) 884–888.
- [14] C. Körner, L. Lehle, K. von Figura, Abnormal synthesis of mannose 1-phosphate derived carbohydrates in carbohydrate-deficient glycoprotein syndrome type I fibroblasts with phosphomannomutase deficiency, *Glycobiology* 8 (2) (February 1998) 165–171.
- [15] E. Krissinel, K. Henrick, Inference of macromolecular assemblies from crystalline state, *J. Mol. Biol.* 372 (2007) 774–797.
- [16] A. Lange, R.E. Mills, C.J. Lange, M. Stewart, S.E. Devine, A.H. Corbett, Classical nuclear localization signals: definition, function, and interaction with importin alpha, *J. Biol. Chem.* 282 (2007) 5101–5105.
- [17] C. Le Bizec, S. Vuillaumier-Barrot, A. Barnier, et al., A new insight into PMM2 mutations in the French population, *Hum. Mutat.* 25 (2005) 504–505.
- [18] G. Matthijs, E. Schollen, E. Van Schaftingen, J.J. Cassiman, J. Jaeken, Lack of homozygotes for the most frequent disease allele in carbohydrate-deficient glycoprotein syndrome type 1A, *Am. J. Hum. Genet.* 62 (3) (1998) 542–550, <https://doi.org/10.1086/301763>.
- [19] B.G. Ng, H.H. Freeze, Perspectives on glycosylation and its congenital disorders, *Trend. Genet.* 34 (6) (2018) 466–476, <https://doi.org/10.1016/j.tig.2018.03.002>.
- [20] R. Niehues, M. Hasilik, G. Alton, et al., Carbohydrate-deficient glycoprotein syndrome type Ib. Phosphomannose isomerase deficiency and mannose therapy, *J. Clin. Invest.* 101 (7) (1998) 1414–1420, <https://doi.org/10.1172/JCI2350>.
- [21] M. Novokmet, E. Lukić, F. Vučković, Ž. Đurić, T. Keser, K. Rajšl, D. Remondini, G. Castellani, H. Gasparović, O. Gornik, G. Lauc, Changes in IgG and total plasma protein glycomes in acute systemic inflammation, *Sci. Rep.* 4 (2014 Mar 11) 4347.
- [22] R. Peanne, P. de Lonlay, F. Foulquier, et al., Congenital disorders of glycosylation (CDG): quo vadis? *Eur. J. Med. Genet.* 61 (2018) 643–663.
- [23] C.H. Rodrigues, D.E. Pires, D.B. Ascher, DynaMut: predicting the impact of mutations on protein conformation, flexibility and stability, *Nucleic Acids Res.* 46 (2018) W350–W355.
- [24] B. Shanti, M. Silink, K. Bhattacharya, et al., Congenital disorder of glycosylation type Ia: heterogeneity in the clinical presentation from multivisceral failure to hyperinsulinaemic hypoglycaemia as leading symptoms in three infants with phosphomannomutase deficiency, *J. Inherit. Metab. Dis.* 32 (2009) 241–251, <https://doi.org/10.1007/s10545-009-1180-2>.
- [25] C.R. Siah, C. Childs, C.K. Chia, K.F.K. Cheng, An observational study of temperature and thermal images of surgical wounds for detecting delayed wound healing within four days after surgery, *J. Clin. Nurs.* 28 (2019) 2285–2295.
- [26] D. Son, A. Harijan, Overview of surgical scar prevention and management, *J. Korean Med. Sci.* 29 (6) (2014) 751.
- [27] C. Thiel, N. Rind, D. Popovici, Hoffmann, et al., Improved diagnostics lead to identification of three new patients with congenital disorder of glycosylation-Ip, *Hum. Mutat.* 33 (2012) 485–487.
- [28] E. Van Schaftingen, J. Jaeken, Phosphomannomutase deficiency is a cause of carbohydrate-deficient glycoprotein syndrome type I, *FEBS Lett.* 377 (1996) 318–320, [https://doi.org/10.1016/0014-5793\(95\)01357-1](https://doi.org/10.1016/0014-5793(95)01357-1).
- [29] S. Vuillaumier-Barrot, G. Hetet, A. Barnier, et al., Identification of four novel PMM2 mutations in congenital disorders of glycosylation (CDG) Ia French patients, *J. Med. Genet.* 37 (8) (2000) 579–580, <https://doi.org/10.1136/jmg.37.8.579T>.
- [30] P. Yuste-Checa, A. Gámez, S. Brasil, L.R. Desviat, M. Ugarte, C. Pérez-Cerdá, B. Pérez, The effects of PMM2-CDG-causing mutations on the folding, activity, and stability of the PMM2 protein, *Hum. Mutat.* 36 (2015) 851–860.